Hindawi
Advances in Civil Engineering
Volume 2021, Article ID 6640167, 9 pages
https://doi.org/10.1155/2021/6640167

Research Article

Flexural Performance of Emulsified-Asphalt-Modified ECC for Expansion Joint Use

Quan Mao,[1] Zhigang Zhang,[2] and Hui Ma[3]

[1]*Jiangsu Xiandai Road & Bridge Co., Ltd., Nanjing 210046, China*
[2]*Key Laboratory of New Technology for Construction of Cities in Mountain Area (Chongqing University), Ministry of Education, Chongqing 400045, China*
[3]*Jiangsu Expressway Engineering Maintenance Technology Co., Ltd., Nanjing 211106, China*

Correspondence should be addressed to Zhigang Zhang; zhangzg@cqu.edu.cn and Hui Ma; huim@seu.edu.cn

Received 22 December 2020; Accepted 6 October 2021; Published 23 October 2021

Academic Editor: Abdulkadir Cuneyt Aydın

The concrete transition zone plays an important role in bridge expansion joint structure, which provides a good connection between the expansion joint installation and bridge decks. However, the premature deteriorations of concrete transition zone are found to be the major diseases of expansion joint during service life. Therefore, a material with high ductility, superior durability, and low modulus/stiffness is highly desired for transition zone. Engineering cementitious composites (ECC), a kind of high-performance concrete featuring the prominent ductility and durability, are a promising material for transition zone of expansion joint. This paper introduces a specific ECC material for transition zone, which is modified by emulsified asphalt (EA-ECC), and has the high deformation ability and low modulus/stiffness. The flexural mechanical properties including flexural stress-load displacement relation, flexural secant stiffness, and elastic modulus of the EA-ECC's matrix were investigated experimentally. The microstructures of EA-ECC were observed via scanning electron microscope (SEM) imaging. Additionally, the influence of test temperature on flexural mechanical properties of EA-ECC was also investigated. It is found that the ultimate flexural stress of EA-ECC reduces gradually with increasing EA content. Conversely, the flexural deformation capacity shows an increasing trend with EA content. Additionally, incorporating EA significantly reduces the flexural secant stiffness and elastic modulus of EA-ECCs. The research results concluded that incorporating EA in ECC can significantly improve the flexural deformation ability accompanied by relatively lower modulus, which is likely to reduce the impact load on transition zone caused by vehicle bumping and prolong the service life of the whole bridge expansion joint structure.

1. Introduction

Expansion joint is an extremely important part in the bridge structure, which is set up to make bridge decks adapt to the deformation caused by the change of temperature and humidity, shrinkage and creep of concrete, bridge pier settlement, beam rotation, etc. Usually, concrete transition zone is set up between expansion joint installation and bridge deck beam, which links the expansion joint installation and bridge beam to make them working together [1]. Unfortunately, expansion joint is the weakest part of a bridge structure. Due to the improper design and construction, the premature destructions of expansion joint usually occurred under the combined action of vehicle load and environmental effects [2]. These destructions could result in the bumping problem when a vehicle passes, which produces an impact load and exacerbates the damage of expansion joints. In addition, the survey found that the damage of concrete transition zone is the greatest destruction of expansion joints, including cracking, spalling, and breakage [3], as shown in Figure 1.

The previous research [4] indicated that there are three main reasons of the premature destructions in concrete transition zone. Firstly, the poor ductility of concrete that is normally used in transition zone cannot make it withstand the repeated deformation between bridge deck beams. Secondly, the poor durability of conventional concrete leads to further deteriorations after initial cracking. The water and

(a) (b) (c)

Figure 1: The destructions of concrete transition zone of expansion joints. (a) Cracking. (b) Spalling. (c) Breakage.

other corrosive chemicals penetrate the concrete transition zone through these cracks, which leads to the corrosion of reinforcements and reduces the bonding between expansion joint and bridge deck beam. In addition, the modulus of conventional concrete transition zone is much larger than that of asphalt pavement on bridge deck, which causes a large impact load when vehicles pass the expansion joint. It is also the reason causing the premature destructions of concrete transition zone. Therefore, a material with high ductility, superior durability, and low modulus/stiffness is highly needed for transition zone of bridge expansion joint. Due to the high compressive and tensile strengths and good durability, ultra-high-performance concrete (UHPC) was considered as a promising material for transition zone of bridge expansion joint [5, 6]. The research of Zhou et al. [7] reported that the UHPC had been applied in bridge expansion joints, such as in United States and Canada. However, the cracking cannot be eliminated completely, which results in the fact that the premature destructions still exist in transition zone [6].

Engineered cementitious composites (ECC), a special kind of high-performance fiber reinforced concrete, were developed by Li and co-workers based on micromechanics and fracture mechanics theory in the 1990s [8, 9]. ECC has excellent mechanical properties and ductility. The compressive strength of ECC could range from 20 to 180 MPa depending on the mix compositions [10–12]. Unlike the brittleness of conventional concrete and strain-softening of fiber reinforced concrete [13], ECC exhibits the metal-like strain-hardening behavior after the first crack occurring, accompanied by multiple microcracks under tensile loading. The typical tensile stress-strain-crack width curve of ECC material under uniaxial tensile load is shown in Figure 2. With the moderate design, the strain capacity of ECC material could reach the range of 3–8%, which is 300–800 times that of conventional concrete and fiber reinforced concrete materials [14, 15]. For conventional concrete and fiber reinforced concrete materials, the limited cracks are localized around the weakest plane of component, and the crack width increases gradually until the failure under the loading. In comparison, the crack width in ECC stabilizes at around 60–100 μm, whilst the number of microcracks increases after tensile strain of

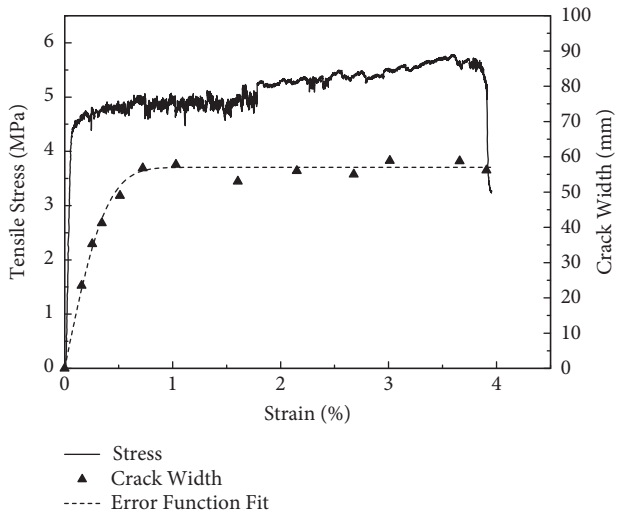

Figure 2: Typical uniaxial tensile stress-strain-crack width curve of ECC [13].

1%. More importantly, the tiny crack width controlled ability is an intrinsic material property of ECC, which is independent of the structure size or external loads [16, 17].

ECC has a prominent durability benefiting from the super tiny crack width. Compared to the cracks (width is in millimeter level) in conventional concrete material, the tiny cracks in ECC dramatically reduce the permeation of water and other corrosive chemicals. What is more, these tiny cracks in ECC can be self-healed due to the continuous hydration of cementitious materials (unhydrated cement and fly ash etc.), pozzolanic reaction of supplemental cementitious materials, and precipitation of $CaCO_3$ under certain circumstances, which significantly recovers the transport and mechanical properties of ECC [18]. The water permeability of cracked ECC was shown to decrease to zero gradually under wet-dry cycle curing condition, accompanied by observation of self-healing products within the cracks [19]. The mechanical properties were also reported to have a significant recovery to almost 100% that of uncracked ECC, such as tensile and flexural strengths, stiffness, and tensile strain capacity [20].

Due to the excellent mechanical properties and durability, ECC is considered as a promising material used in transition zone of bridge expansion joint. In the past two decades, ECC has been successfully applied in bridge engineering field. Lepech and Li [21, 22] conducted the research on applicability of ECC for bridge deck link slabs. The design guidelines and material specifications were developed. Under the collaboration with the Michigan Department of Transportation, the ECC link slab was implemented successfully in 2005, as shown in Figure 3. The expansion joint was removed and replaced with section of ECC overtop the joint. A continuous deck surface was constructed afterwards. Yin et al. [23] studied the shear load-displacement behavior of ECC material in transition zone and reported that ECC has been applied in expansion joints of a steel box girder bridge in Hohhot, China. However, the large elastic modulus discrepancy between of ECC transition zone and asphalt pavement on bridge deck exists. The elastic modulus of ECC is 20000 MPa, while it only ranges from 3000 to 10000 MPa for asphalt pavement material. Accordingly, the huge modulus discrepancy could easily cause the impact load when a vehicle passes the expansion joint, which often leads to the premature damage or destructions in ECC transition zone. Therefore, a specific ECC material with relatively lower modulus/stiffness is needed to be developed for transition zone to prolong the service life of bridge expansion joints.

In previous research, Ma et al. [24] tailored the ECC materials with emulsified asphalt (EA-ECC) for high damping and low modulus. In this study, the EA-ECC material was introduced for transition zone of bridge expansion joints. The schematic diagram of bridge expansion joints using EA-ECC is shown in Figure 4. In the following sections, the influence of EA on the flexural mechanical properties and stiffness of EA-ECCs were investigated through four-point bending test. The elastic modulus of EA-ECC matrix was investigated via uniaxial tensile test. The microstructure of surface between PVA fiber and matrix in EA-ECC was observed via scanning electron microscope (SEM) imaging. Because EA is a thermal sensitive material, the temperature influence on the flexural mechanical properties of EA-ECC was also investigated.

2. Experimental Programs

2.1. Raw Materials. The raw materials used in this study included Portland type I cement CEM-42.5, class F fly ash, fine silica sand, PVA fibers, and styrene-butadiene styrene (SBS) modified emulsified asphalt. In order to control the workability of fresh ECC mixtures, the polycarboxylate-based water reducing admixture (HRWRA) was also used. The chemical components of cement and fly ash are listed in Table 1, which meet the Chinese standards (GB1596-88). The fine silica sand has a mean size of 150 μm. The properties of SBS modified emulsified asphalt are listed in Table 2. The PVA fibers have the size of 12 mm in length and 39 μm in diameter, a tensile strength of 1620 MPa, an elastic modulus of 42.8 GPa, a density of 1.3 g/cm^3, and an elongation of 7%, respectively.

Figure 3: The link slab of bridge decks using ECC material (http://umich.edu/~acemrl/NewFiles/projects/linkslab_timeline.html).

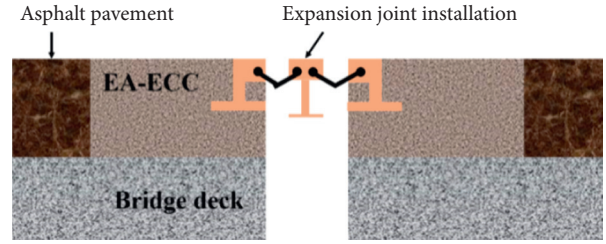

Figure 4: The schematic diagram for EA-ECC transition zone of bridge expansion joint.

2.2. Specimen Preparation. Table 3 lists the mix proportions of different EA-ECC mixtures used in this study. E0 was prepared without EA as a reference mix. The mixtures E1 to E4 were prepared with different EA to cement ratios (EA/C), which is 5%, 10%, 15%, and 25%, respectively. The ratio of fly ash to cement was fixed at 1.2 for all mixtures. Due to the moisture content of 36.8% in EA (solid content of 63.2% listed in Table 2), the ratio of water to cementitious materials (cement and fly ash) was adjusted with EA content for keeping the same water content in all mixtures. The PVA fibers were added by volume fraction of total EA-ECC mixture, which is noted in Table 3.

The EA-ECC mixtures were mixed using a planetary mixer with the capacity of 10 L. Firstly, cement, fly ash, and fine silica sand were dry-mixed for 3 minutes at a low rotation speed of 110 r/min. The mixture of water and EA was then added and mixed for another 5 minutes at a high rotation speed of 198 r/min. In the process of mixing, the HRWRA was added gradually to adjust the fluidity of mortar. The PVA fibers were then added slowly and mixed 10 minutes continually. When the PVA fibers were distributed evenly, the fresh EA-ECC mixture was poured into specific molds. The EA-ECC specimens were demolded after 24 hours and then cured in curing box with the condition of $20 \pm 2^{\circ}$C in temperature and $95 \pm 5\%$ in humidity. All specimens were tested after 28 curing days.

2.3. Test Methods. In this study, the four-point bending test was conducted to investigate the flexural mechanical properties of EA-ECCs, as shown in Figure 5. The EA-ECC specimen has the size of 400 mm in length, 70 mm in width,

Table 1: Chemical components of cement and fly ash (%).

Material	SiO_2	Al_2O_3	Fe_2O_3	CaO	SO_3	P_2O_5	Na_2O	K_2O	TiO_2	MgO
Cement	21.26	7.67	2.88	57.82	4.04	5.26	0	0.78	0.21	—
Fly ash	52.25	27.42	4.84	7.22	1.83	0.89	0.4	1.32	1.1	2.57

Table 2: Properties of SBS modified emulsified asphalt.

Penetration at 25°C (0.1 mm)	Ductility at 25°C (cm)	Soft point (°C)	Sieve residue of 1.18 mm (%)	Storage stability 1 d (%)	Solid content (%)	Standard viscosity C25.3 (s)	Density (g/cm^3)
74	66	49.2	0.03	0.02	63.2	14	1.02

Table 3: Mix proportions of ECCs with different EA contents (weight ratio to cement).

Mix	Cement	Fly ash	Sand	Water	HRWRA	PVA fiber*	EA
E0	1	1.2	0.8	0.55	0.02	2%	0
E1	1	1.2	0.8	0.52	0.02	2%	0.05
E2	1	1.2	0.8	0.49	0.02	2%	0.10
E3	1	1.2	0.8	0.46	0.02	2%	0.15
E4	1	1.2	0.8	0.40	0.02	2%	0.25

Note. *PVA fibers were added by the volume of total ECC mixture.

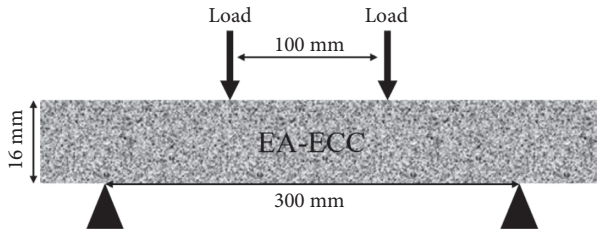

Figure 5: The schematic diagram of four-point bending test on EA-ECC.

and 16 mm in thickness, respectively. The support span of four-point bending test was 300 mm, and middle load point span was 100 mm. The test was conducted under the displacement control at a rate of 1.0 mm/min. During testing, the flexural load and load displacement were recorded. Three specimens were tested for each mix. The elastic modulus of EA-ECC matrix (without PVA fibers) was investigated through uniaxial tensile test. For the details of the uniaxial tensile test, refer to Ma et al. [24]. The scanning electron microscopy (SEM) imaging was also used to observe the microstructures of surface between PVA fibers and matrix.

The influence of temperature on the flexural performances of EA-ECC was investigated using universal testing machine (UTM-25). Firstly, the EA-ECC specimens were cured for 2 hours in the environmental chamber of UTM-25 at different temperatures. The temperature values were selected as 0°C, 25°C, and 60°C, which reflects the most common low temperature, normal temperature, and high temperature, respectively, on road surface in Jiangsu province of China. The four-point bending test was then conducted using UTM-25 at the corresponding temperatures.

3. Results and Discussions

3.1. Flexural Behavior of EA-ECC. Table 4 summarizes the results of four-point bending test on EA-ECCs, including first cracking strength, ultimate flexural stress, and displacement capacity. The flexural stress versus load displacement curves of ECCs with different EA contents are shown in Figure 6. In Table 4, the first cracking strength (the first stress drop-off of the flexural stress-load displacement curve) has a reduction trend with increasing EA content. It reduces from 6.17 MPa to 4.06 MPa, with EA content increasing from 0 to 25%. The first cracking strength of ECC material is mainly governed by the matrix fracture strength. Due to incorporating EA, the network structure of cementitious hydration products (C-S-H) was obstructed by asphalt membrane in composite [25]. According to Fu et al. [26], more air bubbles enter the CA mortar during the mixing process, with EA content increasing. Similarly, the porosity of EA-ECC matrix increases with EA content, which results in the relatively lower fracture strength of EA-ECC matrix. Therefore, the EA-ECC with higher EA content has a lower first cracking strength.

The ultimate flexural stress of EA-ECCs has a similar reduction trend with increasing EA content. It is reduced by 40% when EA content increases from 0 to 25%. The flexural/tensile strength of ECC material is governed by the fiber bridging capacity on the weakest crack plane. According to Li and Leung [8], the fiber bridging capacity is closely related to interfacial bond between fiber and matrix, including chemical bonding (G_d) and frictional bond strength (τ_0). According to the previous research of Ma et al. [24], the chemical bonding G_d and frictional bond strength τ_0 of EA-ECC showed a decreasing trend with incorporating EA. The chemical bonding G_d is governed by the metal cation concentration, in particular Al^{3+} and Ca^{2+}, in the interfacial transition zone (ITZ) between PVA fibers and matrix [27]. The frictional bond strength τ_0 is closely related to the roughness and compactness of ITZ [28]. Due to incorporating EA, the asphalt membrane was formed on ITZ in EA-ECCs, which may reduce the metal cation concentration and the roughness of ITZ. In addition, as can be seen in Figure 7, the PVA fiber surface in E4 remains intact after being pulled out, while it is damaged obviously in E0. It also indicates that incorporating EA could reduce the frictional bond strength. Therefore, the reduction of chemical bonding and frictional bond strength with increasing EA content results in a lower

Table 4: Flexural mechanical properties of EA-ECCs under four-point bending test.

Mix	First cracking strength	Ultimate flexural stress	Deflection capacity
E0	6.17 ± 0.54 MPa	11.87 ± 0.34 MPa	9.01 ± 0.77 mm
E1	5.67 ± 0.78 MPa	9.57 ± 0.81 MPa	18.32 ± 3.34 mm
E2	6.53 ± 0.31 MPa	9.01 ± 0.05 MPa	17.15 ± 1.05 mm
E3	5.43 ± 0.42 MPa	9.15 ± 0.19 MPa	26.60 ± 1.95 mm
E4	4.06 ± 1.02 MPa	7.13 ± 0.71 MPa	33.32 ± 2.65 mm

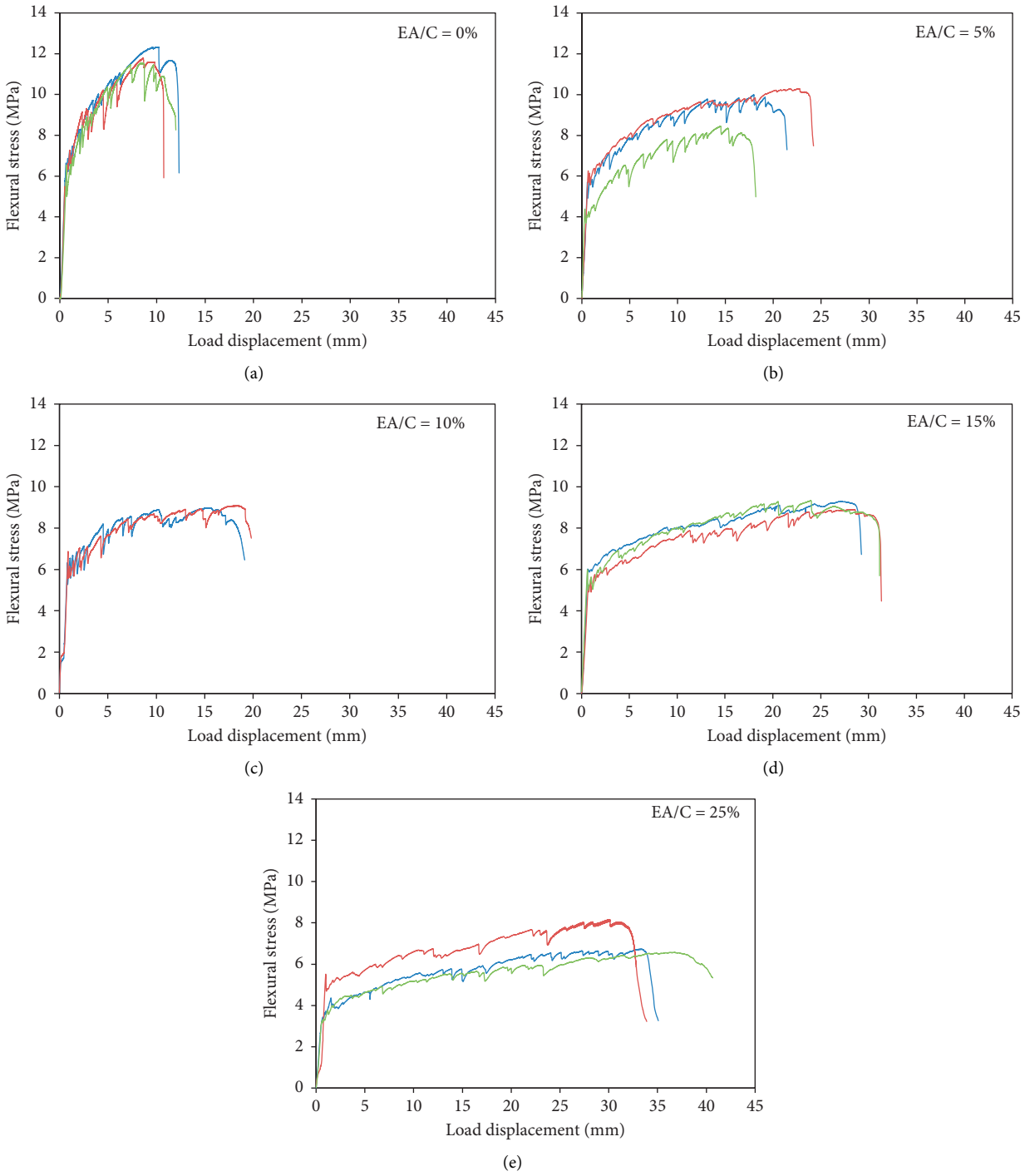

Figure 6: Typical flexural stress versus load displacement curves of EA-ECCs: (a) E0; (b) E1; (c) E2; (d) E3; (e) E4.

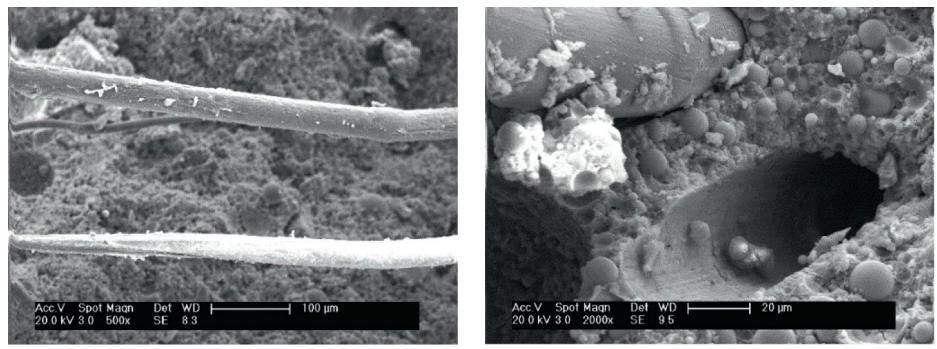

(a) (b)

Figure 7: Surface conditions of PVA fibers and matrix in ECCs: (a) E0; (b) E4.

fiber bridging capacity, and subsequently a lower ultimate flexural stress of EA-ECCs compared to E0.

Conversely, the flexural displacement capacity has a significant improvement with increasing EA content. The load displacement of E4 reaches 33 mm, which increases by 2.67 times compared to that of E0. In order to acquire strain-hardening behavior in ECCs, the strength criterion and energy criterion should be satisfied [29], which are shown in equations (1) and (2).

$$\sigma_{fc} \leq \sigma_0, \tag{1}$$

$$J_{\text{tip}} \leq j_b', \tag{2}$$

where σ_{fc} and σ_0 are matrix fracture strength and fiber bridging capacity, respectively; J_{tip} and J_b' are crack tip toughness and complementary energy of fiber bridging stress-crack opening width relation, respectively. The pseudo-strain-hardening performance (PSH) indexes were proposed by Li [9] to quantitatively evaluate strain-hardening behavior of ECC, which are shown in the following equation:

$$\text{PSH}_{\text{energy}} = \frac{J_b'}{J_{\text{tip}}} \& \text{PSH}_{\text{strength}} = \frac{\sigma_0}{\sigma_{fc}}. \tag{3}$$

According to Ma et al. [24], the PSH indexes have an observably increasing trend with EA content increases. It means that these criterions can be satisfied with larger margin, which results in the larger flexural deformation capacity of EA-ECCs with higher EA content.

The flexural toughness is another important parameter for evaluating the flexural mechanical properties of ECC materials. It represents the energy absorption capacity of ECC component before failure under flexural loading. In this study, the flexural toughness of ECC is demonstrated by toughness index, which is defined as the ratio of integral area under the whole flexural stress-load displacement curve with abscissa to the area before first cracking, as shown in Figure 8. Using this method, the toughness index of ECC and EA-ECCs is calculated and shown in Figure 9. As can be seen, overall, the toughness index of EA-ECCs except for E2 is obviously larger than that of E0. For the profit from the larger toughness, EA-ECC transition zone could absorb more energy under vehicle loading instead of brittle fracture, which greatly prolongs the service life of expansion joint.

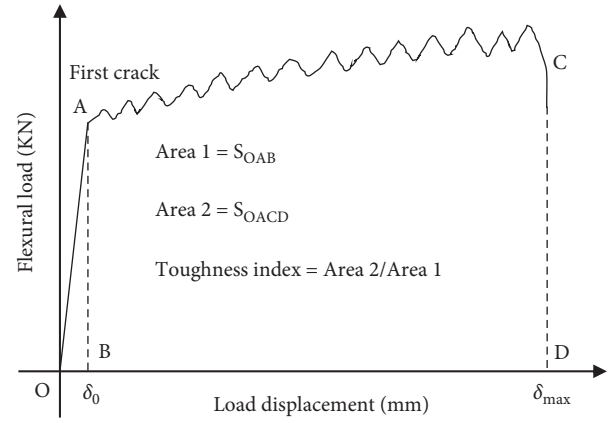

Figure 8: The schematic diagram of flexural toughness index of EA-ECC.

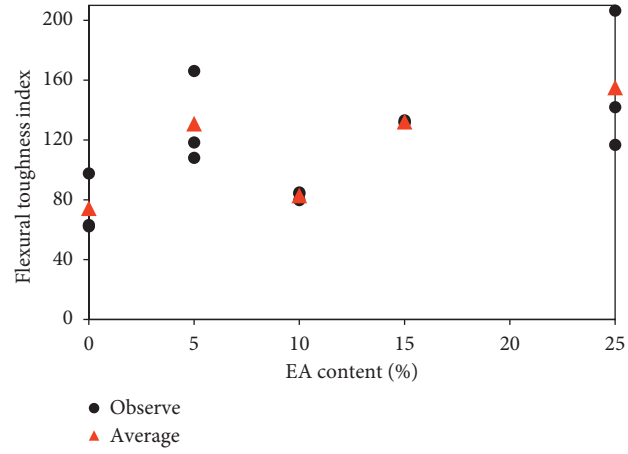

Figure 9: The flexural toughness of EA-ECCs with different EA contents.

3.2. Stiffness of EA-ECC. In this study, the secant modulus of flexural stress-load displacement relation in the elastic stage (before the first cracking point) was used to investigate the

influence of EA on flexural stiffness of EA-ECC. The secant modulus is defined as the slope between the origin and first cracking point in flexural stress-load displacement curve, as illustrated in Figure 10. The flexural secant modulus of EA-ECCs with different EA contents is presented in Figure 11. As can be seen, the flexural secant moduli are similar when EA content increases from 0 to 10%, while it drops significantly after continually increasing EA content to above 10%. Due to the viscoelasticity of asphalt and asphalt membrane retarding the link of cement hydration production, the matrix of EA-ECC could generate a larger deformation before cracking, which results in a relatively lower stiffness of composite.

The tensile elastic modulus of EA-ECC matrixes, obtained from uniaxial tensile test on matrix specimen, as a function of EA content, is shown in Figure 12. As can be seen, the elastic modulus of ECC matrix has a significant reduction after incorporating EA, while it stabilizes with subsequently increasing EA content from 10% to 25%. The elastic modulus of matrix without EA is about 15000 MPa, while it is only 4500 MPa for the matrix with EA; it decreases by 70%. Normally, stone matrix asphalt (SMA) concrete is the most used material for bridge deck pavement. The elastic modulus of SMA ranges from 3000 MPa to 6000 MPa [30], which is similar with that of EA-ECC matrix. The results indicate that incorporating EA in ECC observably reduces the modulus discrepancy between asphalt pavement on bridge deck and EA-ECC transition zone. It could relieve the vehicle bumping problem and reduce the accompanying impact load on EA-ECC transition zone, which reduces the possibility of premature deteriorations occurring and then prolongs the service life of expansion joint.

3.3. Temperature Effects on Flexural Mechanical Properties. In this section, the mix E2 was used to investigate the influence of test temperature on flexural mechanical properties. Typical flexural stress-load displacement curves of E2 under different test temperatures are shown in Figure 13. As can be seen, it has the largest ultimate flexural stress and first cracking strength accompanied by the lowest flexural displacement at low temperature of 0°C. The ultimate flexural stress can reach 18 MPa, while the displacement capacity is only 10 mm. When test temperature increases to 25°C, the ultimate flexural stress and first cracking strength have a significant decrease, while the displacement capacity increases observably. The ultimate flexural stress and first cracking strength decrease by 55% and 45% compared to those at 0°C, while the displacement capacity increases by 44%. When the test temperature sequentially increases to 60°C, the ultimate flexural stress and first cracking strength have a slightly decrease, while the displacement capacity increases a little bit compared to that at 25°C. The flexural toughness indexes of E2 at different test temperatures are shown in Figure 14. The toughness index increases by 2.9 times when the test temperature increases from 0°C to 60°C.

Due to the thermal sensitivity, EA can be hardened at low temperature of 0°C. The frozen asphalt phase in EA-ECC can form a strong network, which leads to a higher fracture

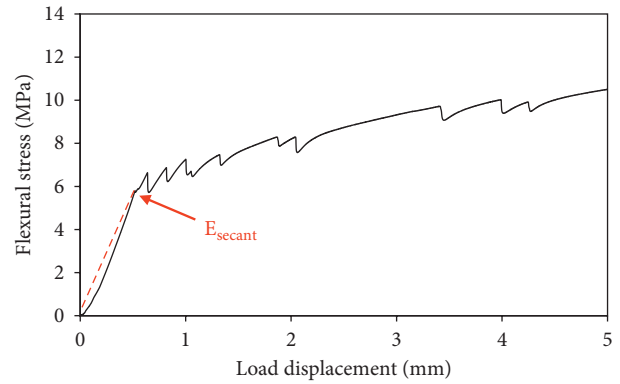

Figure 10: The secant stiffness definition of flexural stress-load displacement curve.

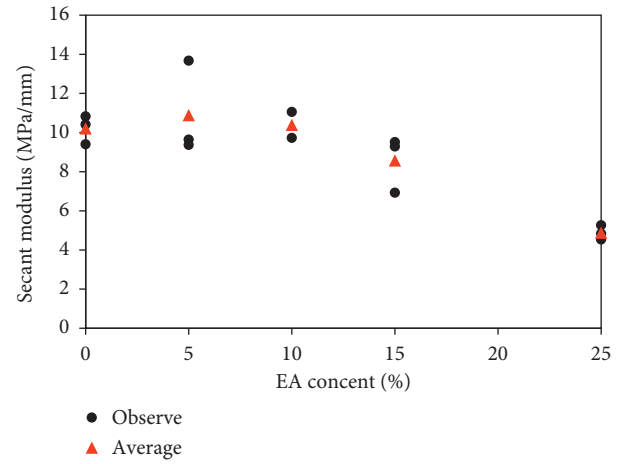

Figure 11: The secant modulus of EA-ECCs with different EA contents.

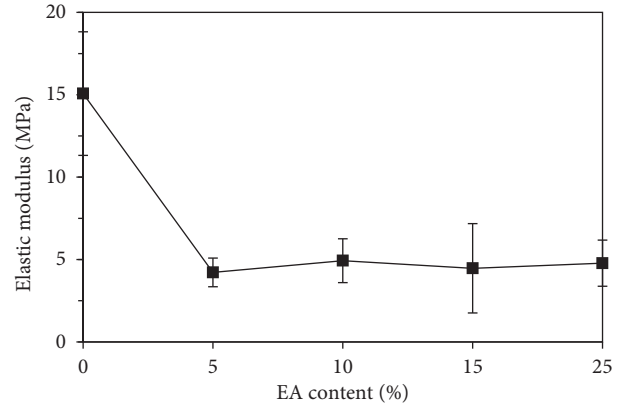

Figure 12: Elastic modulus of EA-ECC matrixes with different EA contents.

strength of matrix. The hardened asphalt phase improves the adhesive between asphalt and cement hydration products, which also increases the fracture strength of matrix and subsequently first cracking strength. As described previously, the fiber bridging capacity is closely related to interfacial bond between fiber and matrix. The hardened asphalt phase increases the roughness of ITZ, which results

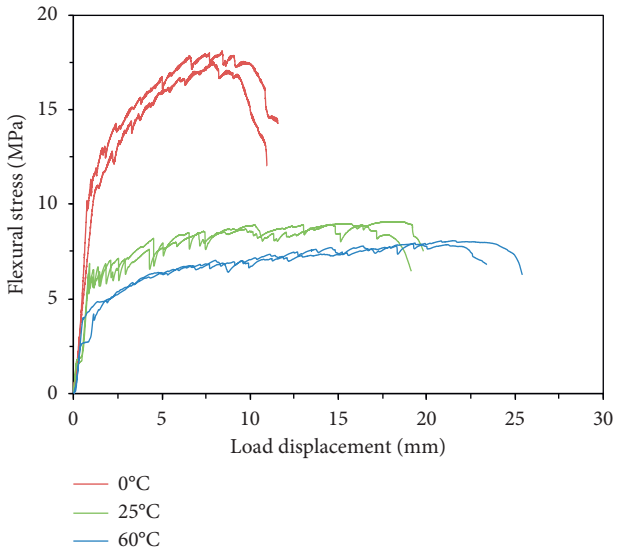

Figure 13: Flexural stress-load displacement curves of E2 at different test temperatures.

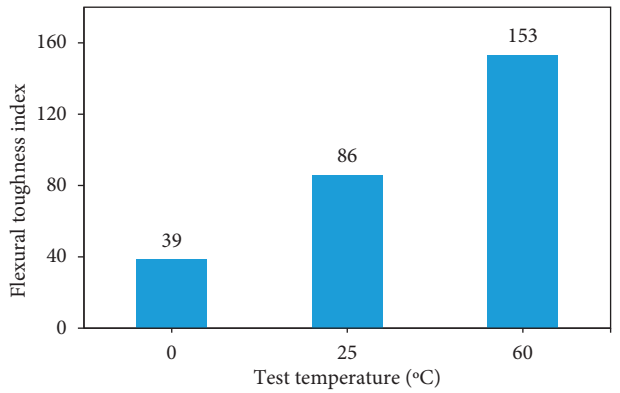

Figure 14: The flexural toughness index of E2 at different test temperatures.

in a higher frictional bond and subsequently ultimate flexural stress at low temperature. Conversely, the hardened asphalt phase increases the bond between fiber and matrix and hardness of interface, which increases the difficulty of fiber pullout and the possibility of fiber rupture. Therefore, EA-ECC has a relatively smaller flexural deformation under lower temperature.

The flexural secant modulus of E2 under different temperatures is shown in Figure 15. As can be seen, the flexural secant modulus is reduced significantly with increasing temperature. Due to the viscoelasticity of asphalt, the asphalt phase in EA-ECC has a softening trend with increasing temperature, and the viscidity is dominant for asphalt. The higher viscidity of asphalt in EA-ECC allows the matrix to generate a larger deformation before first cracking, which leads to a smaller flexural stiffness of EA-ECC under higher temperature.

The above results indicated that, under low temperature, the larger modulus of EA-ECC transition zone causes a relatively obvious vehicle bumping and larger impact load,

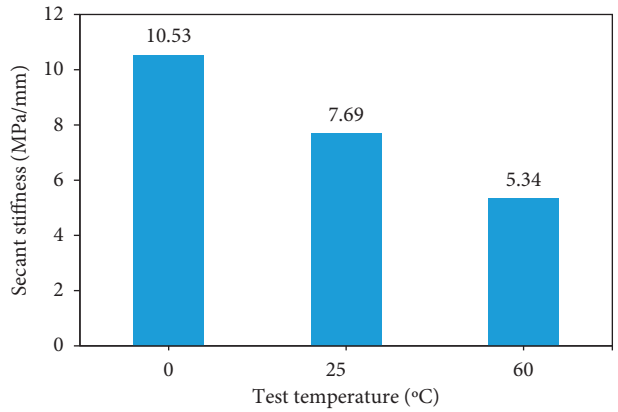

Figure 15: The flexural secant modulus of E2 at different test temperatures.

while it could bear larger load without cracking. On the contrary, EA-ECC transition zone could absorb more energy from vehicle loading at higher temperature, such as in summer.

4. Conclusions

In this study, a special ECC modified by emulsified asphalt (EA-ECC) was introduced to be used in transition zone of bridge expansion joint. The flexural mechanical properties of EA-ECCs, including flexural stress-load displacement relation and stiffness, were investigated experimentally. The temperature influences on flexural behavior of EA-ECC were also investigated. The following conclusions can be drawn based on the research findings in this study.

(1) Incorporating emulsified asphalt could significantly reduce the modulus of ECC while maintaining the excellent mechanical properties. The low rigidity of EA-ECC material highly probably improves the vehicle bumping problem and therefore reduces the impact load on EA-ECC transition zone.

(2) The flexural deformation of EA-ECC increases significantly, while the ultimate flexural stress is reduced obviously with EA content increasing. Nevertheless, the ultimate flexural stress of E4 still reaches a value above 7 MPa, which could satisfy the requirement of transition zone application.

(3) The flexural mechanical properties of EA-ECC are influenced by temperature significantly. The E2 exhibits smaller ultimate flexural stress, first cracking strength, and larger displacement capacity and flexural toughness accompanied by a smaller flexural stiffness under higher temperature.

Data Availability

The data are available upon request.

Conflicts of Interest

The authors declare that they have no conflicts of interest.

Acknowledgments

The authors would like to graciously thank the National Natural Science Foundation of China (Grant no. 52078083), the Fundamental Research Funds for the Central Universities (2021CDJQY-008), 111 Project of China (Grant no. B18062), Natural Science Foundation Project of Chongqing (cstc2020jcyj-msxmX0901), and the Transportation Science Research Project of Jiangsu Province (No. 2019Y71) for the financial support of this work.

References

[1] T. Guo, L. Y. Huang, J. Liu, and Y. Zou, "Damage mechanism of control springs in modular expansion joints oflong-span bridge," *Journal of Bridge Engineering*, vol. 23, no. 7, pp. 1–11, 2018.

[2] P. D. Mascio, G. Loprencipe, L. Moretti, L. Puzzo, and P. Zoccali, "Bridge expansion joint in road transition curve: Effects assessment on heavy vehicles," *Applied Sciences*, vol. 7, no. 6, p. 599, 2017.

[3] L.-M. Chang and Y.-J. Lee, "Evaluation of performance of bridge deck expansion joints," *Journal of Performance of Constructed Facilities*, vol. 16, no. 1, pp. 3–9, 2002.

[4] Y. Yang, "Research of rapid repair materials for bridge expansion joints rehabilitation," Doctoral Dissertation, Chongqing Jiaotong University, Chongqing, China, 2017.

[5] S. S. G. Balakumaran, K. O'Neill, T. C. Springer, and A. Matteo, "Elastomeric concrete plug joints: a new durable bridge expansion joint design," *Transportation Research Record: Journal of the Transportation Research Board*, vol. 2642, no. 1, pp. 18–25, 2017.

[6] L. Ren, M. Y. Liang, K. Wang, Y. He, and G.-G. Zhao, "Key performance and application of ultra-high- performance concrete in bridge expansion joint," *Bulletin of the Chinese Ceramic Society*, vol. 37, no. 6, pp. 2048–2052, 2018.

[7] M. Zhou, W. Lu, J. Song, and G. C. Lee, "Application of ultra-high performance concrete in bridge engineering," *Construction and Building Materials*, vol. 186, pp. 1256–1267, 2018.

[8] V. C. Li and C. K. Y. Leung, "Steady-state and multiple cracking of short random fiber composites," *Journal of Engineering Mechanics*, vol. 118, no. 11, pp. 2246–2264, 1992.

[9] V. C. Li, "From micromechanics to structural engineering - the design of cementitious composites for civil engineering application," *Journal of Structure Engineering/Earthquake Engineering*, vol. 10, no. 2, pp. 37–48, 1993.

[10] R. Ranade, V. C. Li, M. D. Stults, W. F. Heard, and T. S. Rushing, "Composite properties of high-strength, high-ductility concrete," *ACI Materials Journal*, vol. 110, no. 4, pp. 413–422, 2013.

[11] F. Qin, Z. Zhang, Z. Yin, J. Di, L. Xu, and X. Xu, "Use of high strength, high ductility engineered cementitious composites (ECC) to enhance the flexural performance of reinforced concrete beams," *Journal of Building Engineering*, vol. 32, Article ID 101746, 2020.

[12] Z. Zhang, J.-C. Liu, X. Xu, and L. Yuan, "Effect of sub-elevated temperature on mechanical properties of ECC with different fly ash contents," *Construction and Building Materials*, vol. 262, Article ID 120096, 2020.

[13] V. C. Li, S. X. Wang, and C. Wu, "Tensile strain-hardening behavior of polyvinyl alcohol engineered cementitious composite (PVA-ECC)," *ACI Materials Journal*, vol. 98, no. 6, pp. 483–492, 2001.

[14] Z. Zhang, F. Qin, H. Ma, and L. Xu, "Tailoring an impact resistant engineered cementitious composite (ECC) by incorporation of crumb rubber," *Construction and Building Materials*, vol. 262, Article ID 120116, 2020.

[15] Z. Zhang, F. Yang, J.-C. Liu, and S. Wang, "Eco-friendly high strength, high ductility engineered cementitious composites (ECC) with substitution of fly ash by rice husk ash," *Cement and Concrete Research*, vol. 137, Article ID 106200, 2020.

[16] H. Ma and Z. Zhang, "Paving an engineered cementitious composite (ECC) overlay on concrete airfield pavement for reflective cracking resistance," *Construction and Building Materials*, vol. 252, Article ID 119048, 2020.

[17] Z. Zhang, S. Liu, F. Yang, Y. Weng, and S. Qian, "Sustainable high strength, high ductility engineered cementitious composites (ECC) with substitution of cement by rice husk ash," *Journal of Cleaner Production*, vol. 317, p. 128379, 2021.

[18] Z. Zhang, J. Hu, and H. Ma, "Feasibility study of ECC with self-healing capacity applied on the long-span steel bridge deck overlay," *International Journal of Pavement Engineering*, vol. 20, no. 8, pp. 884–893, 2019.

[19] Z. Zhang, Q. Zhang, and V. C. Li, "Multiple-scale investigations on self-healing induced mechanical property recovery of ECC," *Cement and Concrete Composites*, vol. 103, pp. 293–302, 2019.

[20] H. Ma, E. Herbert, M. Ohno, and V. C. Li, "Scale-linking model of self-healing and stiffness recovery in Engineered Cementitious Composites (ECC)," *Cement and Concrete Composites*, vol. 95, pp. 1–9, 2019.

[21] M. D. Lepech and V. C. Li, "Application of ECC for bridge deck link slabs," *Materials And Structures*, vol. 42, no. 9, pp. 1185–1195, 2009.

[22] M. D. Lepech and V. C. Li, "Sustainable pavement overlays using engineered cementitious composites," *International Journal of Pavement Research and Technology*, vol. 3, no. 5, pp. 241–250, 2010.

[23] L. Q. Yin, S. G. Liu, C. W. Yan, J. Zhang, and X. Wang, "Shear load-displacement curves of PVAFiber-reinforced engineered CementitiousComposite expansion joints in steel bridges," *Applied Sciences*, vol. 9, no. 24, pp. 1–13, 2019.

[24] H. Ma, S. Qian, and V. C. Li, "Tailoring engineered cementitious composite with emulsified asphalt for high damping," *Construction and Building Materials*, vol. 201, pp. 631–640, 2019.

[25] Q. Wang, P. Y. Yan, A. Ruhan, J. Yang, and X. Kong, "Strength mechanism ofcement-asphalt mortar," *Journal of Materials in Civil Engineering*, vol. 23, no. 9, pp. 1353–1359, 2011.

[26] Q. Fu, Y. Xie, G. Long, D. Niu, and H. Song, "Dynamic mechanical thermo-analysis of cement and asphalt mortar," *Powder Technology*, vol. 313, pp. 36–43, 2017.

[27] S. X. Wang and V. C. Li, "Engineered cementitious composites with high-volume fly ash," *ACI Materials Journal*, vol. 104, no. 3, pp. 233–241, 2007.

[28] E. H. Yang, Y. Z. Yang, and V. C. Li, "Use of high volumes of fly ash to improve ECCmechanical properties and material greenness," *ACI Materials Journal*, vol. 104, no. 6, pp. 620–628, 2007.

[29] E.-H. Yang, S. Wang, Y. Yang, and V. C. Li, "Fiber-bridging constitutive law of engineered cementitious composites," *Journal of Advanced Concrete Technology*, vol. 6, no. 1, pp. 181–193, 2008.

[30] Q. Xue, X.-t. Feng, L. Liu, Y.-j. Chen, and X.-L. Liu, "Evaluation of pavement straw composite fiber on SMA pavement performances," *Construction and Building Materials*, vol. 41, pp. 834–843, 2013.